Preliminary Assessment of sCO_2 Radial Compressor Design on the N_s-D_s Diagram Using the KAIST-TMD code

Seungkyu Lee [a], Jeong Ik Lee[a*]
[a]*Dept. Nuclear & Quantum Eng., KAIST, 373-1, Guseong-dong, Yuseong-gu, Daejeon, 305-701, Republic of Korea*
[*]*Corresponding author: jeongiklee@kaist.ac.kr*

Keywords : sCO_2, Radial compressor, Ns-Ds diagram, specific speed, specific diameter

1. Introduction

The development of small modular reactors (SMRs) and micro modular reactors (MMR) has increased the importance for marine propulsion and data center electricity consumption. The supercritical carbon dioxide (sCO_2) Brayton cycle has been considered as a promising power conversion option for nuclear applications because it can achieve a compact system configuration while maintaining competitive thermal efficiency at moderate turbine inlet temperatures [1]. In addition, the high density of sCO_2 enables a substantial reduction in turbomachinery size compared with conventional gas-cycle systems.

Radial compressors are commonly considered for the main compressor of sCO_2 Brayton cycles. Preliminary selection and sizing of turbomachinery has performed with non-dimensional parameters specific speed (Ns), and specific diameter (Ds). Balje organized experimental and design experience for pumps, compressors, and turbines into the well-known (Ns-Ds) diagram, in which turbomachinery type, achievable efficiency, and characteristic size can be estimated from dimensionless parameters [2]. The diagram has remained an important preliminary-design tool because it allows the feasible design region to be identified before detailed aerodynamic design is performed. However, the original Balje diagram was primarily established from water and air turbomachinery experience available machine technologies. Its efficiency contours therefore should reflect fluid properties and aerodynamic design development. Several studies have shown that the contours have changed when turbomachinery is operated with non-conventional working fluids [3], [4], [5].

Near the critical point, CO_2 exhibits a high density and strong real-gas property variations. Therefore, sCO_2 turbomachinery operate at a relatively high Reynolds number while low Mach numbers compared with conventional gas compressors of similar power. Previous studies have demonstrated that the thermophysical behavior of sCO_2 near the critical point significantly affects compressor design and performance prediction. Consequently, similarity relationships developed primarily from conventional air and water based turbomachinery data should be reassessed before being directly applied to sCO_2 compressors.

The present study uses the validated the KAIST-TMD code framework to reconstruct Ns-Ds efficiency contour for an sCO_2 radial compressor. The resulting efficiency contours are compared with the original Balje's radial compressor contour [2]. The objective is to evaluate whether the conventional Balje map reproduces the design trends predicted for a high density real gas sCO_2 compressor.

2. Methods

2.1 Design screening and similarity parameters

The compressor condition was selected from the main compressor condition of an sCO_2 recompression Brayton cycle for a 100 MW heat source. The compressor inlet temperature was set to 35 degree Celsius, because closer to the CO_2 critical temperature can make possibility of local condensation and inlet temperature control difficult. The corresponding compressor inlet pressure and mass flow rate were 8.4 MPa and 332.9 kg/s, respectively. The outlet pressure of the first stage becomes 14.5 MPa with maximum pressure as 25 MPa.

The dimensionless specific speed and specific diameter are defined as Equation 1. Here, Q is the inlet volumetric flow rate, Δh is the isentropic enthalpy rise, ω is the angular speed, and D_2 is the impeller outlet diameter. Since Q and Δh are fixed, each RPM corresponds to one N_s, whereas C_a and β modify the resulting geometry, D.

$$N_s = \frac{\omega\sqrt{Q}}{\Delta h^{3/4}} \quad D_S = \frac{D_2 \Delta h^{1/4}}{\sqrt{Q}} \qquad (Equation\ 1)$$

For the prescribed thermodynamic boundary condition, Q and Δh are fixed. Consequently, Ns is determined directly by rotational speed. The design RPM range was selected such that Ns varied from 0.2 to 1.0, because this range corresponds to the radial compressor region in the Balje Ns-Ds diagram. At each Ns, the meridional inlet velocity, Ca, and impeller backswept angle, β_2, were varied to generate different impeller outlet diameters and corresponding Ds values. Design point and screening steps of variable parameters are listed in Table I. Fig. 1 shows the Balje's original Ns-Ds diagram for various types of compressors and pumps

Table I: Design point and screening parameter of a radial compressor

Parameter	Value
Working fluid / stage	CO_2 / 1stage
Mass flow rate	332.9 kg/s
Tin	308.15 K

Pin / Pout	8.4 / 14.5 MPa
Ca (diameter screening)	5-120 m/s, Δ=5
Rotational Speed	2,200-15,000, Δ=200
Backswept angle β_2	0-70˚, Δ=5˚

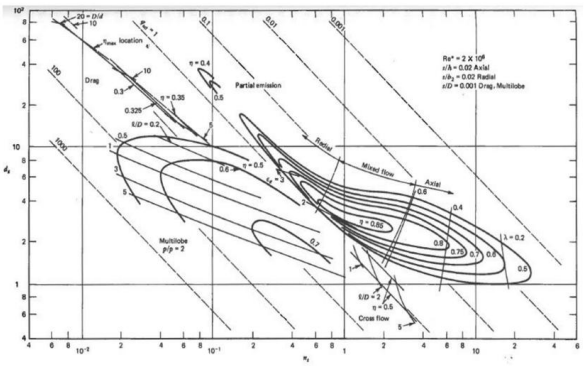


Fig. 1. Balje's original compressor and pump Ns-Ds diagram

2.2 The KAIST-TMD code and loss model set

The KAIST-TMD code is a 1-D turbomachinery design code developed to account for following characteristics. Real-gas thermodynamic properties are adopted using the REFPROP database, with an enthalpy-based Euler work relation rather than an ideal-gas approximation. This methodology was developed to retain applicability to fluids with strong non-ideal behavior near the critical point. This design code has been assessed against experimental sCO_2 compressor data in previous studies [1,6].

The predicted performance of a 1-D turbomachinery model depends strongly on the selected loss correlations. Therefore, an arbitrary combination of loss correlations can make significant difference. Cho et al. suggested 'Oh set' as proper combinations of radial compressor loss models validated with sCO_2 radial compressor experimental data of pressure ratio and efficiency [7]. Therefore, 'Oh set' is adopted in the KAIST-TMD code in this study and its individual loss models and proposers are shown in Table II.

Table II: Loss models adopted for the sCO_2 radial compressor analysis

Loss model	Proposer
Incidence loss	Conrad
Blade loading loss	Coppage
Skin friction loss	Jansen
Clearance loss	Jansen
Mixing loss	Johnston and Dean
Leakage loss	Aungier
Recirculation loss	Oh
Disk friction loss	Daily and Nece

3. Results

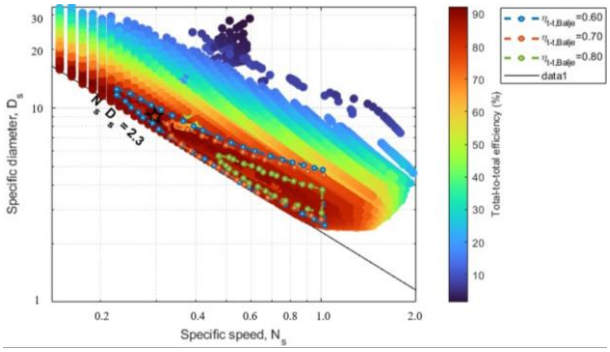


Fig. 2. KAIST-TMD efficiency results on the Ns-Ds plane with realistic lower limit of Ns*Ds, and Balje's efficiency contour

Fig. 2 shows the radial compressor design space obtained from the KAIST-TMD parameter screening. The calculated design points were projected onto the Ns-Ds plane, and the isentropic efficiency is indicated by color. For a Ns, which corresponds to a rotational speed, variations in Ca and the impeller backswept angle, β_2, produce a range of Ds values and compressor efficiencies.

The screening results show a clear efficiency distribution in the Ns-Ds plane. At a given Ns, the calculated efficiency generally increases as Ds decreases toward the lower boundary of the feasible design region. The feasible design points do not extend indefinitely toward smaller Ds, but approach a lower boundary approximately described by $Ns * Ds = 2.3$.

This value is close to the theoretical radial compressor limit of $Ns * Ds = 2$. The difference between the theoretical and calculated boundaries is reasonable because the theoretical relation represents an ideal geometric limit, whereas the KAIST-TMD calculation includes finite aerodynamic. Therefore, the efficiency remains approximately 80% or higher near this calculated lower boundary. In Balje's original Ns-Ds diagram, the iso-efficiency lines for 50–80% also overlap in this region. Considering this, it explains why the KAIST-TMD code was not designed for values of Ns*Ds ranging from 2.0 to 2.3.

Based on the parameter screening results, 60%, 70%, and 80% efficiency contours were extracted in the design space as shown in Fig. 2. For each Ns, the maximum Ds satisfying each efficiency level was selected to construct the upper efficiency envelope.

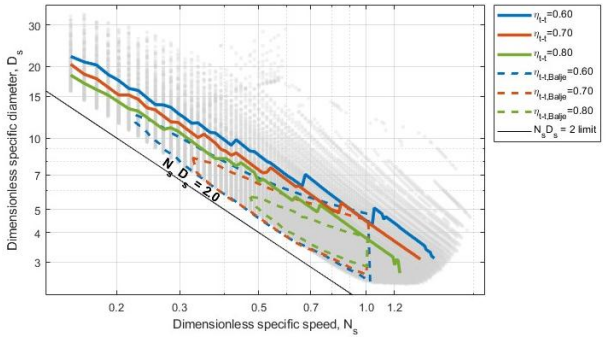


Fig. 3. KAIST-TMD efficiency envelopes compared with the digitized Balje radial compressor Ns-Ds diagram.

Figure 3 compares the upper efficiency envelopes obtained from the KAIST-TMD code with the original Balje radial-compressor map. The calculated 60%, 70%, and 80% contours show the same first order tendency as the Balje contours. Ds decreases monotonically with increasing Ns, and the upper boundary moves toward smaller Ds as the efficiency level increases. The KAIST-TMD upper envelopes are represented as Equations 2 to 4.

$$D_{s,60\%} = 4.6891 N_s^{-0.825},\ R^2 = 0.9969\ (Equation\ 2)$$
$$D_{s,70\%} = 4.4159 N_s^{-0.788},\ R^2 = 0.9968\ (Equation\ 3)$$
$$D_{s,60\%} = 3.8861 N_s^{-0.811},\ R^2 = 0.9978\ (Equation\ 4)$$

The similar exponents and high R^2 values indicate that the three efficiency boundaries follow a consistent power-law relationship. The 60% contour forms the outermost boundary, followed by the 70% and 80% contours. The calculated contours are generally located at larger Ds than the original Balje contours, particularly in the low-Ns region, while the difference decreases as Ns increases.

The present results suggest that the 60%, 70%, and 80% curves can be represented as upper efficiency boundaries. For example, the 80% curve represents the largest Ds at which approximately 80% isentropic efficiency is obtained for a given Ns. Moving toward smaller Ds from this upper boundary generally results in higher efficiency until the practical lower design boundary is reached. The same interpretation applies to the 70% and 60% curves.

4. Conclusions and Future works

A parameter screening of an sCO_2 radial compressor was performed using the KAIST-TMD code, and the calculated design space was projected onto the Ns-Ds plane. Variations in rotational speed, axial velocity, and impeller backswept angle produced a systematic efficiency distribution, from which the 60%, 70%, and 80% efficiency boundaries were obtained.

The KAIST-TMD code screening showed that compressor efficiency generally increases as Ds decreases at a given Ns, until the feasible design space approaches an effective lower boundary of approximately $Ns * Ds = 2.3$. This value is close to the theoretical radial compressor limit of $Ns * Ds = 2.0$, and efficiencies of approximately 80% or higher were maintained near the calculated boundary.

The resulting upper efficiency envelopes followed power law relationships with $R^2 > 0.996$ and reproduced the overall decreasing trend of Ds with increasing Ns in the original Balje diagram. However, unlike the closed efficiency contours in the conventional Balje map, the KAIST-TMD results did not show a lower iso-efficiency line. The 60%, 70%, and 80% curves are therefore more appropriately interpreted as upper efficiency boundaries, with the lower side of the design region constrained by the radial compressor Ns Ds limit.

These results indicate that the conventional Balje diagram remains useful for describing the overall similarity trend of radial compressors, while the detailed efficiency contour representation may require reassessment for real-gas turbomachinery.

Balje's original Ns-Ds diagram was plotted using the pressure-based loss model available at the time. The compressor working fluid at that time had a compressibility factor of approximately 1.0, whereas the compressibility factor of sCO_2 in this study is approximately 0.24. Therefore, the Ns-Ds diagram plotted by Balje may differ from the one generated by the KAIST-TMD code. In future research, it is necessary to vary the fluid inlet compressibility factor conditions to investigate how the compressibility factor affects the shape of the Ns-Ds diagram. Furthermore, when plotting the Ns-Ds diagram using the KAIST-TMD code, the iso-efficiency curve is significantly influenced by the loss models. Therefore, while some loss categories are dominant and others are not, it should be examined how these losses vary on the Ns-Ds plane.

ACKNOWLEDGEMENT

This work was supported by the National Research Foundation of Korea (NRF) grant funded by the Korea government (MSIT) (No.: RS-2024-00436693).

REFERENCES

[1] J. Lee, J. I. Lee, H. J. Yoon, and J. E. Cha, "Supercritical Carbon Dioxide Turbomachinery Design for Water-Cooled Small Modular Reactor Application," *Nuclear Engineering and Design*, Vol. 270, pp. 76–89, 2014.
[2] O. E. Balje, *Turbomachines: A Guide to Design, Selection, and Theory*, Wiley-Interscience, New York, 1981.
[3] R. Capata and E. Sciubba, "Experimental Fitting of the Re-Scaled Balje Maps for Low-Reynolds Radial Turbomachinery," *Energies*, Vol. 8, pp. 7986–8000, 2015.
[4] V. Mounier, L. E. Olmedo, and J. Schiffmann, "Small Scale Radial Inflow Turbine Performance and Pre-Design Maps for Organic Rankine Cycles," *Energy*, Vol. 143, pp. 1072–1084, 2018.
[5] M. Masi, L. Da Lio, and A. Lazzaretto, "An Insight into the Similarity Approach to Predict the Maximum Efficiency of Organic Rankine Cycle Turbines," *Energy*, Vol. 198, 117278, 2020.
[6] J. Lee, S. K. Cho, and J. I. Lee, "The Effect of Real Gas Approximations on S-CO_2 Compressor Design," *Journal of Turbomachinery*, Vol. 140, 051007, 2018.
[7] S. K. Cho, S. Son, J. Lee, S. W. Lee, Y. Jeong, B. S. Oh, and J. I. Lee, "Optimum Loss Models for Performance Prediction of Supercritical CO_2 Centrifugal Compressor," *Applied Thermal Engineering*, Vol. 184, 116255, 2021.
[8] S. K. Cho, S. J. Bae, Y. Jeong, J. Lee, and J. I. Lee, "Direction for High-Performance Supercritical CO_2 Centrifugal Compressor Design for Dry Cooled Supercritical CO_2 Brayton Cycle," *Applied Sciences*, Vol. 9, 4057, 2019.